INTERNATIONAL JOURNAL OF CLIMATOLOGY
Int. J. Climatol. (2015)
Published online in Wiley Online Library
(wileyonlinelibrary.com) DOI: 10.1002/joc.4560

Climate change and water resources in a tropical island system: propagation of uncertainty from statistically downscaled climate models to hydrologic models

Ashley E. Van Beusekom,[a*] William A. Gould,[a] Adam J. Terando[b] and Jaime A. Collazo[c]

[a] *USDA Forest Service, International Institute of Tropical Forestry (IITF), Río Piedras, Puerto Rico,*
[b] *U.S. Geological Survey, Department of the Interior Southeast Climate Science Center, Raleigh, NC, USA*
[c] *U.S. Geological Survey North Carolina Cooperative Fish and Wildlife Research Unit, Department of Applied Ecology, North Carolina State University, Raleigh, NC, USA*

ABSTRACT: Many tropical islands have limited water resources with historically increasing demand, all potentially affected by a changing climate. The effects of climate change on island hydrology are difficult to model due to steep local precipitation gradients and sparse data. This work uses 10 statistically downscaled general circulation models (GCMs) under two greenhouse gas emission scenarios to evaluate the uncertainty propagated from GCMs in projecting the effects of climate change on water resources in a tropical island system. The assessment is conducted using a previously configured hydrologic model, the Precipitation Runoff Modelling System (PRMS) for Puerto Rico. Projected climate data and their modelled hydrologic variables versus historical measurements and their modelled hydrologic variables are found to have empirical distribution functions that are statistically different with less than 1 year of daily data aggregation. Thus, only annual averages of the projected hydrologic variables are employed as completely bias-corrected model outputs. The magnitude of the projected total flow decreases in the four regions covering Puerto Rico, but with a large range of uncertainty depending on the makeup of the GCM ensemble. The multi-model mean projected total flow decreases by 49–88% of historical amounts from the 1960s to the 2090s for the high emissions scenarios and by 39–79% for the low emissions scenarios. Subsurface flow contributions decreased the least and groundwater flow contributions decreased the most across the island. At locations critical to water supply for human use, projected streamflow is shown to decrease substantially below projected withdrawals by 2099.

KEY WORDS future water supply; general circulation models; hydrology; Precipitation Runoff Modelling System; Puerto Rico; statistical downscaling; tropical island hydrology

Received 5 January 2015; Revised 13 October 2015; Accepted 13 October 2015

1. Introduction

Understanding the potential consequences of climate change for water resources is critical for national, regional, and local decision-makers. Global studies find that current water use is probably unsustainable, but point out large regional and local uncertainties depending on climatic and human consumption trajectories (Alcamo *et al.*, 2007; Hejazi *et al.*, 2013). Furthermore, water management decisions are made on a smaller scale than global, thus water resource projections at regional scales are needed to inform decisions. Regional studies are especially needed in the tropics, because humid tropical regions have high hydrological energy inputs and are therefore likely to have higher rates of hydrologic-induced transformation resulting from climate change (Huntington, 2006; Wohl *et al.*, 2012). Any reduction in water resources could result in serious consequences for these regions because many island systems are dependent on surface waters for domestic, industrial, agricultural, and energy needs as well as for maintaining ecosystem functions. In addition, limited available land, high population densities, and often-inadequate governmental resources add to the challenge of managing water (Bonell *et al.*, 2005).

There are many difficulties in developing much-needed hydrologic models of future streamflow in these systems. The steep topography found on many tropical islands results in rapid runoff that is highly variable both in space and time (Bonell *et al.*, 2005). The complexity of tropical island runoff is compounded by the fact that rainfall often varies drastically over short distances. Across Puerto Rico for example (an island located in the northeast Caribbean), annual rainfall can consistently vary from less than 1 m to nearly 5 m over distances of 10–15 km (Daly *et al.*, 2003). Hydrologic models are driven by regional-scale downscaled climate projections that are relied upon to provide detailed information that global-scale general circulation models (GCMs) cannot resolve. Because the regional-scale downscaled climate projections are highly uncertain, especially when trained on only sparse climatic data, it is imperative to develop the hydrologic projections

* Correspondence to: A. E. Van Beusekom, USDA Forest Service, Jardín Botánico Sur, 1201 Calle Ceiba, International Institute of Tropical Fore. E-mail: beusekom@usgs.gov

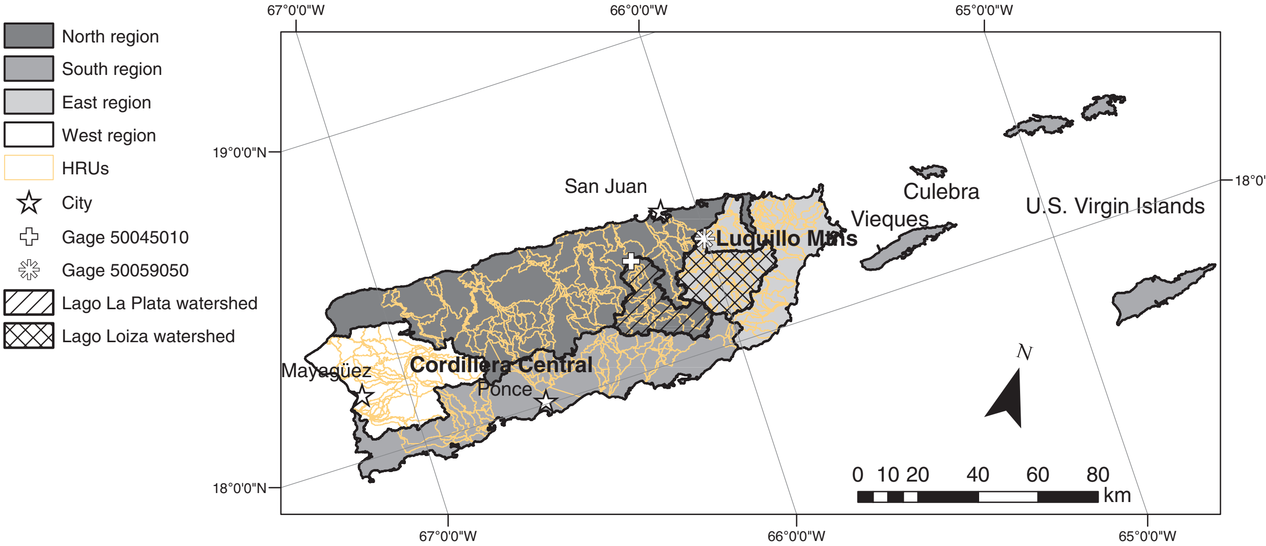

Figure 1. Map of Puerto Rico with geographic locations. The black lines on each map divide the island into four climate regions and the HRUs are outlined.

with a reliable temporal resolution (Chen *et al.*, 2012; Hay *et al.*, 2014). This process is neither straightforward nor simple and can involve layers of modelling wherein assumptions and uncertainty are propagated along the chain of processes (Pappenberger and Beven, 2006). The ideal outcome of the modelling effort is new information that sheds light on possible consequences of climate change along with an understanding of the uncertainty and the potential value of this information for further research and decision-making. The uncertainty cascade in the assessment of climate change impacts starts with the emission scenarios, and propagates downward to the GCM initial conditions, the GCM model structure, and the downscaling technique, and further to the hydrologic model structure and hydrologic model parameters (Wilby and Harris, 2006; Addor *et al.*, 2014; Vano *et al.*, 2014). This study does not attempt to address the entire uncertainty cascade, but addresses an important and manageable component using a top-down uncertainty assessment with a pre-existing hydrologic model.

This study projects changes in water resources for the tropical island of Puerto Rico after assessing the uncertainty propagated from statistically downscaled GCMs to a hydrologic model. A distributed-parameter process-based hydrologic model was previously configured and calibrated for Puerto Rico using historical climate and streamflow data (Van Beusekom *et al.*, 2014). In this study, hydrologic fluxes from the hydrologic model driven by climate projections are compared to the hydrologic fluxes from the model driven by climate observations, and the results are used to present the most reliable temporal resolution of the hydrology under two climate change scenarios. Future hydrology is examined at locations critical to the water supply on the island to explore the possible timing of hydrological regime changes that would result in substantial consequences for water use and management.

2. Study area

Puerto Rico is the smallest of the Greater Antilles Islands, located in the northeastern Caribbean Sea. The main island is approximately 8900 km^2 with a thin strip of coastal plains, 8–16 km wide, surrounding steep igneous upland. Orographic effects are a major control on temperature and precipitation. There are four mountain ranges within Puerto Rico (Figure 1). Three of these mountain ranges comprise the Cordillera Central, which has a maximum elevation of 1300 m. Maximum elevation of the Luquillo Mountain range, where the highest annual rainfall occurs, is 1100 m. These mountain ranges naturally divide Puerto Rico into four climatic regions: a moderately wet region north of the Cordillera Central, a dry region south of the Cordillera Central, a wet region east of the Cordillera Central surrounding the Luquillo Mountains, and a moderately wet region west of the Cordillera Central (Van Beusekom *et al.*, 2014).

Puerto Rico follows the Caribbean weather pattern created by the easterly trade winds from the Atlantic Ocean. In general, the Caribbean rainfall season is bimodal, with an early rainfall season from May to June and a late rainfall season from August to November. The island-wide dry season is from January to April. The rainfall seasons are a result of the eastward extension of a warm pool of sea surface temperature, with the dry season onset occurring when the North Atlantic Subtropical High (NASH) pressure system extends into the region and suppresses convection (Giannini *et al.*, 2000). Much of the short-term climatic variability is driven by ENSO (El Niño-Southern Oscillation) events (Angeles *et al.*, 2007). Temperatures in Puerto Rico are fairly constant spatially and temporally (Daly *et al.*, 2003).

In Puerto Rico, over 85% of public water supply comes from surface waters, most of which are stored in reservoirs (Molina-Rivera and Gómez-Gómez, 2008). Population on the island has been decreasing since 1998, but water use has continued to grow (Molina-Rivera and Gómez-Gómez, 2008). The locations for new reservoirs on the island are limited with the best hydrological sites already occupied (Hunter and Arbona, 1995). The largest city, San Juan, gets most of its water from two of these reservoirs: Lago La Plata, built in 1974, with a drainage area of 291 km^2; and Lago Loíza (also known as Lago Carraizo) built in 1953, with a drainage area of 331 km^2 (http://pr.water.usgs.gov/public/rt/pr_lakes). In 1995, about 35% of the drinking water came from Lago La Plata and 49% from Lago Loíza (Angulo *et al.*, 2011). See watersheds and locations in Figure 1.

Island-wide water-use allocation pressures exerted on these water resources to meet competing human and environmental needs are tremendous. In past years during periods of pronounced drought, reduced streamflow resulted in hundreds of millions of dollars in agricultural losses and year-long water rationing that caused public health concerns for hundreds of thousands of people (Larsen, 2000). Furthermore, it is advisable that some streamflow is allowed to reach the ocean in order to maintain coastal riparian continuity for migratory aquatic species, maintain the health of mangrove and other wetlands and the ecosystem functions they provide, maintain recreational and cultural resources, and maintain viable populations of amphidromous fish species (Cintron *et al.*, 1978; Neal *et al.*, 2009; Cooney and Kwak, 2013). Adequate levels to maintain sustainable habitats and other ecosystem services provided by freshwater have been systematically quantified in only a few watersheds (Benstead *et al.*, 1999).

3. Methods

3.1. Climate input for the hydrologic model

Previously in Van Beusekom *et al.* (2014), a hydrologic model was configured with measured station data (MSD) of daily precipitation and maximum and minimum temperature from 46 weather stations in the National Weather Service Cooperative Observer Network across Puerto Rico. A multiple linear regression method (Hay *et al.*, 2006) was used by Van Beusekom *et al.* (2014) to spatially distribute the daily climate data (measured or projected) from the observing network locations to each hydrologic response unit (HRU) in Puerto Rico based on the longitude, latitude, and elevation of the HRU, with different coefficients for each month.

The coefficients in the regression model were derived using mean monthly climate variables calculated at each HRU using Parameter-elevation Regressions on Independent Slopes Model (PRISM; Daly *et al.*, 2003) data. The coefficients have been derived using historical climate station data. The method using PRISM was implemented because of the poor quantity and quality of the available data. Several dominant regression relations in Puerto Rico were found with the PRISM data. These were consistent with the four climatic regions defined by the mountain ranges described earlier. Therefore, Puerto Rico was divided into four climatic regions (referred to as the North, South, East, and West) and regression equations were calculated for each of the four regions (see Figure 1 for geographic outlines of the regions). Other researchers have identified similar climate regions in Puerto Rico (e.g. Carter and Elsner, 1997; Harmsen *et al.*, 2004). The four climatic regions resulted in four separate hydrologic models for Puerto Rico that were parameterized and calibrated. The total drainage areas for the North, South, East, and West regions are 3700, 2625, 1265, and 1632 km^2, respectively. Owing to the greater areal extent of the North region, changes in surface-water flow in the North region will have the largest impact on total flow for Puerto Rico. For more information see Van Beusekom *et al.* (2014).

The projected daily climate variables used as inputs must be derived from downscaled GCMs because the original GCMs cannot resolve local precipitation gradients. The two primary downscaling approaches, statistical and dynamical, introduce different types of uncertainties and biases (Fowler *et al.*, 2007). Dynamical downscaling uses the output from GCMs to provide the boundary conditions for higher resolution numerical models, thus making it possible to simulate climate variables at a high resolution and also to explicitly resolve more atmospheric processes (such as convection) and dynamic features (e.g. hurricanes; Zhao *et al.*, 2009). However, dynamical downscaling is computationally expensive, and any large GCM biases will still be retained. To date, dynamical downscaling has not been performed at the spatial resolution necessary to resolve the convective processes that are responsible for most precipitation on Puerto Rico.

Statistical downscaling assumes that a stationary (i.e. time invariant) relationship exists between global and regional climate characteristics, which can be used to build an empirical model to predict local climate characteristics based on coarse-scale GCM output (Fowler *et al.*, 2007). This method is much less computationally expensive than dynamical downscaling and therefore can more easily be deployed across large ensembles of GCMs. Statistical downscaling allows for more robust characterizations of GCM structural uncertainty (Terando *et al.*, 2012). However GCM biases, such as inaccurate temporal Caribbean precipitation patterns from using coupled atmosphere–ocean GCM outputs (discussed in Ryu and Hayhoe, 2013), could also be propagated to the local downscaled output. Furthermore, tropical islands pose serious challenges for the successful deployment of statistical downscaling techniques due to the sparse meteorological station network, steep precipitation gradients, poor data quality, and the lack of a definitive mechanistic relationship between large-scale atmospheric predictors and local precipitation (Bonell *et al.*, 2005; Douville *et al.*, 2006; Gutmann *et al.*, 2014).

Stoner *et al.* (2013) statistically downscaled GCM output to increase the resolution of the climate projections to Puerto Rico weather station locations using the Asynchronous Regional Regression Model (ARRM). The ARRM is based on quantile regression, which matches quantiles of the observed and simulated time series, while

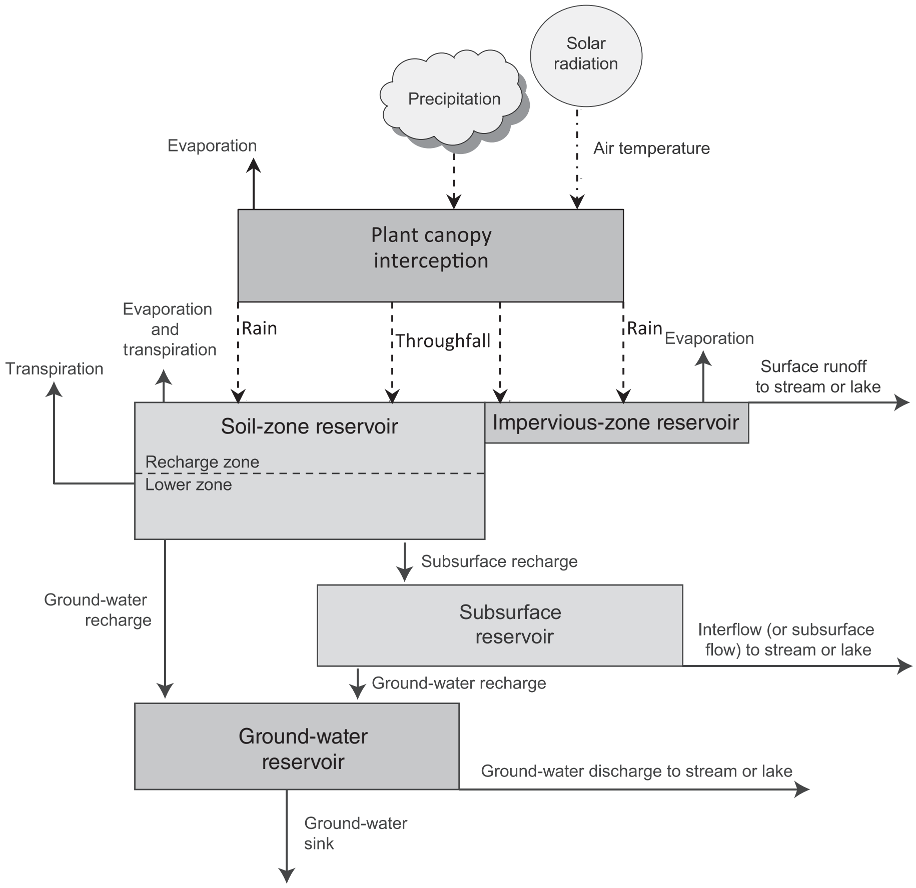

Figure 2. Overview of the PRMS conceptualization of basin components and fluxes (Source: Markstrom *et al.*, 2008).

also using a piecewise regression model to improve reproduction of extremes in the daily distribution (Koenker and Bassett, 1978). For precipitation, a mixture model clustering approach that includes non-homogeneous transition probabilities to model the occurrence and intensity of daily precipitation was used (Vrac and Naveau, 2007).

For this study, the ARRM outputs from ten GCMs (CCSM, CGCM3_T47, CGCM3_T63, CNRM, ECHAM5, ECHO, GFDL_2.0, GFDL_2.1, HADCM3, and PCM), developed as part of the Third and Fourth Assessment Reports of the Intergovernmental Panel on Climate Change (IPCC; Nakicenovic *et al.*, 2000), were used, with two greenhouse gas emissions scenarios, A2 (higher future emissions) and B1 (lower future emissions). The ARRM outputs only exist at those weather station locations that met the downscaling culling criteria of more than 3650 total observations and more than 200 observations for each of the 12 months in the MSD from 1980 to 1999. As a result, ARRM outputs are not available for 18 of the 46 observing stations for temperature and downscaled precipitation values are not available for 6 of the 46 stations. However, the available stations are still evenly distributed over the island.

3.2. Hydrologic model overview

The Precipitation Runoff Modelling System (PRMS) was used to simulate land-surface hydrologic processes in Puerto Rico, including evapotranspiration, runoff, infiltration, interflow, and soil moisture on the basis of spatially distributed daily inputs of precipitation and maximum and minimum temperature, as well as land cover and other characteristics as documented in Van Beusekom *et al.* (2014). PRMS is a modular, deterministic, distributed-parameter, process-based hydrologic model used to simulate the generation of streamflow from surface flow, subsurface flow, and groundwater flow contributions (Figure 2). The reader is referred to Leavesley *et al.* (1983) and Markstrom *et al.* (2008) for a complete description of PRMS. Model results are calibrated to match measured daily stream gage flows, mean monthly solar radiation, and monthly potential evapotranspiration data. A multi-step, multi-objective function scheme is used to calibrate water balance, daily timing, daily high and low flows, incoming solar radiation, and potential evapotranspiration, for physically based parameters that have a range of plausible values (Hay and Umemoto, 2006). Owing to large reported error for the streamflow, a ‘best gage’ was selected for each region based on model ability to reproduce monthly water balances, and the (daily) PRMS model was calibrated with error bars on this gage for each region. The use of dynamic land cover parameters over static ones was shown to improve the model performance. For more details, see Van Beusekom *et al.* (2014).

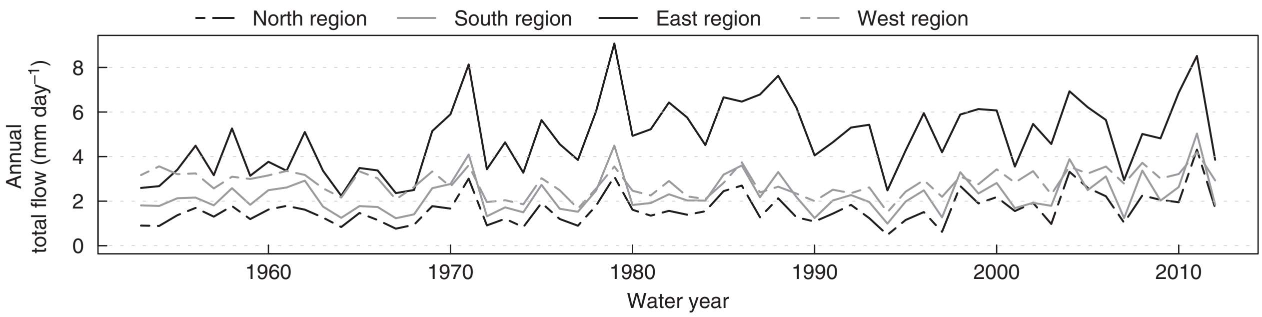

Figure 3. Annual simulated total flow using MSD and dynamic land cover parameters for the North, South, East, and West regions.

The spatially distributed parameter capabilities of PRMS are provided by partitioning the watershed into HRUs (Figure 1). The HRUs are determined by defining a set of Points of Interest (POIs; stream gages, reservoir and lake outflows, and major river confluences), aggregating the minimally sufficient set of flow lines needed to connect each hydrologically consecutive pair of POIs into a single routing segment, and dividing the local contributing area associated with the segment into 'left-bank' and 'right-bank' HRUs (Viger and Bock, 2014). For the PRMS application there are 489 HRUs over the four hydrologic regions. Each HRU is assumed to be homogeneous with respect to its hydrologic response. PRMS is conceptualized as a series of reservoirs (soil zone, shallow subsurface, and groundwater; see Figure 2) whose outputs combine to produce runoff. For each HRU, a water balance is computed each day and an energy balance is computed twice a day. Surface, subsurface, and groundwater flows from each HRU are routed to an associated stream network for total flow. Once in the network, water is routed to the basin outlet (or the coast, in the case of this study). In this paper, total flow is the total local flow produced at each geographical location, and streamflow is the routed total flow through each geographical location (depth of flow versus rate of flow).

Van Beusekom *et al.* (2014) showed that the PRMS model performance improved in basins that were highly modified (by humans) when dynamic land cover change was implemented. Thus, in this study the models driven with the MSD and ARRM use dynamic land cover input with parameters changing on a yearly basis until year 2012. After 2012, the land cover is held constant, as there are no currently available future projections of land cover. The magnitude of the historical interannual variability for each region can be seen in Figure 3 for total flow for years 1953–2012 using MSD and dynamical land cover (see Figure S1, Supporting Information for the details of the flow components). Flow shown includes water that routes directly to the ocean without routing to a stream first, where it would be more readily useable as drinking water. Van Beusekom *et al.* (2014) excluded flow that routes directly to the ocean. In the North region, 26% of the area routes directly to the ocean; in the South region, 59%; in the East region, 22%; and in the West region, 13% (this does not mean this percentage of regional flow routes directly to the ocean as each ocean-routed HRU contributes different amounts of flow to the regional flow on a daily basis).

3.3. Differences in variables from models driven with historical climate and with downscaled GCMs

To evaluate the differences in models driven with historical climate and those driven with downscaled GCMs, the daily climate variables (maximum temperature, minimum temperature, precipitation) from the ARRM outputs downscaled from the ten GCMs and from the MSD were spatially distributed to the 489 HRUs with the multiple linear regression method previously described (Van Beusekom *et al.*, 2014), for the period spanning 1961–1999. The calibrated hydrologic model in each region (North, South, East, and West) was then run for each of the ten climate models and the observations with 1 year of model initialization, resulting in the comparison of 14 244 days of hydrologic variables (total flow, surface flow, subsurface flow, and groundwater flow) for each HRU. Then, the estimated shape parameters (mean, variance, skewness, kurtosis) of the empirical distributions of the ARRM versus MSD-driven hydrologic model output were compared. The comparison was used to identify potential sources of uncertainties, and uncertainties in projected hydrologic changes.

The non-parametric two-sample Kolmogorov–Smirnov (KS) test (Conover, 1971) was used to evaluate how many days of each historical climate and hydrologic variable in each HRU must be aggregated to accept the null hypothesis that the datasets resulting from the MSD and the ARRM are from identical populations (Hay *et al.*, 2014). The KS test finds the maximum distance between two empirical cumulative distribution functions, and is sensitive to differences in both central tendency and distribution shape. In this study, the null hypothesis was rejected if the p-value was less than 0.01. Ties in the non-continuous distributions were resolved using the permutation method which adds a small amount of noise to the data (Præstgaard, 1995). The KS test results supplied a measure of the temporal resolution of the models driven by the ARRM, and also allowed for selection of models to include in the ensemble 'best flow GCMs'. Those included are the GCMs in which the KS tests comparing MSD-driven PRMS models and the ARRM-driven PRMS models reported p-values of 0.01 or greater for all flow variables (total, surface, subsurface, and

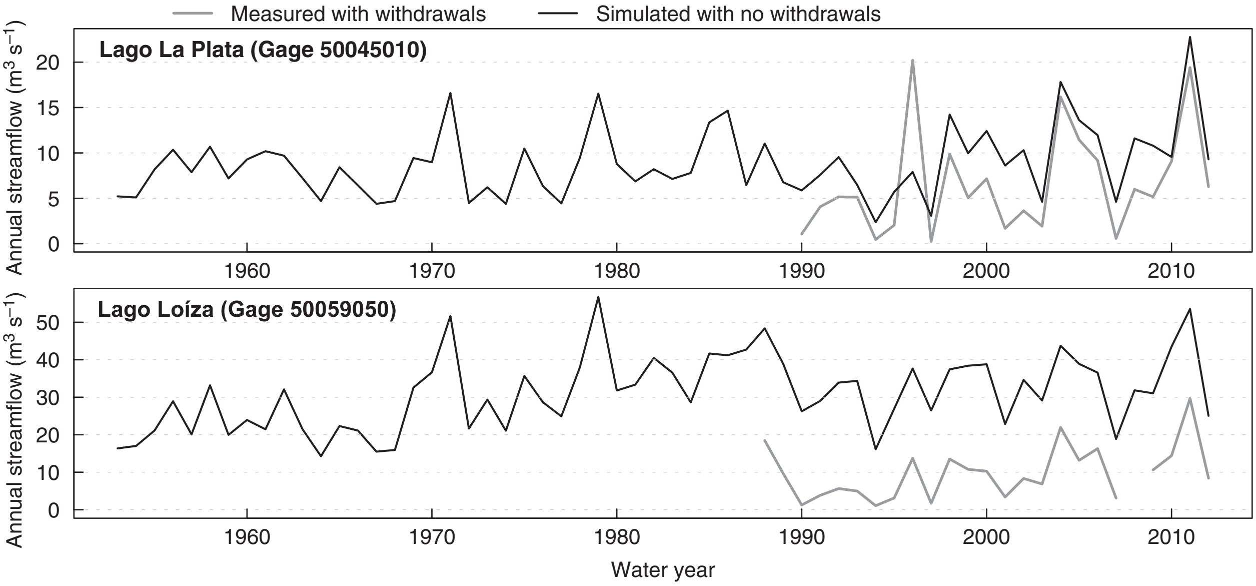

Figure 4. Annual simulated streamflow using MSD and dynamic land cover parameters and measured streamflow at gages at dams on Lago La Plata and Lago Loíza. The measured streamflow includes withdrawals and the simulated streamflow does not include withdrawals.

groundwater flow) in at least 75% of the region in a year of data aggregation or less.

3.4. Climate model ensembles for driving PRMS simulations

PRMS simulations for each region were run with the ARRM and ensemble averages of the annual flow variable outputs were calculated for years 1962–2099 for the A2 and B1 scenarios. Because there is large uncertainty in GCMs it is recommended to always use some ensemble of GCMs (not a single GCM) (Todd *et al.*, 2011), and to present the range of GCMs for a simplified measure of the uncertainty in the projections (Stainforth *et al.*, 2007). Three types of ensembles were used that represent the tradeoffs between maximizing ensemble size to better characterize structural uncertainty across GCMs, and maximizing the accuracy of the ensemble projection by culling models that fail to meet some criteria. The three ensemble combinations used to calculate model-averaged annual flow for Puerto Rico consisted of (1) all GCMs ($n=10$), (2) only the GCMs culled to 'best flow GCMs' as determined by KS tests in each region ($n=0$, 2, or 5 depending on the region), and (3) only the GCMs culled to 'bimodal precipitation GCMs' (n = 2) as determined by those that simulate the timing and magnitude of the bimodal seasonal cycle of Puerto Rico precipitation (Ryu and Hayhoe, 2013). The year 1961 was used to initialize the PRMS model. Ten-year moving averages of the annual projections were calculated, so that the long-term trends were apparent.

3.5. Estimated withdrawals at critical water supply locations

In order to explore future water supply at critical locations, the projected withdrawals at the reservoirs of Lago La Plata and Lago Loíza were estimated and the projected streamflow leaving the reservoirs was simulated. The measured streamflow leaving each reservoir at the gages for years 1953–2012 is shown in Figure 4, which necessarily includes withdrawals. The simulated historical streamflow using MSD and dynamic land cover parameters at USGS gages 50045010 and 500059050 at dam sites on Lago La Plata (a point on the river before the dam was built) and Lago Loíza, respectively, are also shown in Figure 4. The streamflow leaving each reservoir was simulated without upstream and reservoir withdrawals, which are unknown. This figure shows the magnitude of the historical interannual variability in the streamflow at these locations, as well as allowing for an estimation of the withdrawals upstream of the two gages for the common overlap period between simulation and observations, years 1990–2012.

4. Results

4.1. Differences and temporal resolution of hydrologic models driven by downscaled GCMs

The empirical distributions of the HRU-temperatures derived from the MSD and ARRM have similar shape parameters (Table 1). However, the ARRM outputs downscaled from most GCMs and in most HRUs over-predict the mean amount of historic precipitation from the MSD, and the ARRM outputs downscaled from all GCMs and in all HRUs have very high variance compared with the historic precipitation from the MSD. These shape biases are propagated through the hydrologic variables of total flow and the components of surface, subsurface, and groundwater flow (Table 1).

The shape differences in each percentile of the empirical distributions of precipitation are largest for the North

Table 1. Summary of distribution shape biases in models using MSD and ARRM.

Variable	Median HRU AARM-MSD difference for average of all downscaled GCMs			
	Mean	Variance	Skewness	Kurtosis
Maximum temp.	0.13 °C	0.68 °C^2	−0.04 °C^3	0.08 °C^4
Minimum temp.	0.16 °C	0.98 °C^2	0.01 °C^3	0.05 °C^4
Precipitation	2%	76%	−29%	−52%
Total flow	22%	85%	−30%	−47%
Surface flow	20%	77%	−30%	−49%
Subsurface flow	18%	137%	−26%	−41%
Groundwater flow	60%	135%	5%	16%

region by absolute value but are similar, in direction by percentile across all regions (Figure 5). Model biases of zero in the lower percentiles (≤30th percentile) indicate that at least 30% of the days are dry for both the MSD and ARRM outputs. The ARRM results show increasing positive median biases from the 30th to the 60th percentile, indicating that the ARRM simulations tend to overestimate the smaller events relative to the MSD. The larger precipitation events (events greater than the 80th percentile) are also overestimated by the ARRM.

The distributions of (modelled and observed) daily precipitation and hydrologic flow have positively skewed distributions because there are numerous zero events and no upper bound on infrequent large events (i.e. hurricanes), thus they have long tails to the right (Mielke and Johnson, 1974). The ARRM daily precipitation and modelled flow variables (except groundwater) are less positively skewed than the MSD, meaning the ARRM variables are more symmetric than MSD (Table 1, for more details see Figure S4). In the unimodal case, the probability density function of a distribution with large kurtosis has a sharper peak and fatter tails, compared with the probability density function of a distribution with smaller kurtosis. The ARRM daily precipitation has smaller kurtosis than the MSD (Table 1, for more details see Figure S5). Similarly, the ARRM-driven models of flow variables (except groundwater) have smaller kurtosis than MSD-driven models of flow variables. There is much more variety among the groundwater flow empirical distribution shape parameters for the different GCMs (for more details see Figures S2–S5).

The KS test of differences between MSD and ARRM distributions for the total flow variable resulted in large differences across the island and between GCMs for the required amount of temporal aggregation to achieve a p-value of 0.01 or greater (Figure 6). Many areas require temporal aggregation of 1 year or more to achieve a p-value of 0.01 or greater (and thus accept the null hypothesis of no difference between the distribution functions). For temperature, the required temporal aggregation is less in many regions compared with the hydrologic variables and precipitation (for more details see Figure S6). For precipitation, more temporal aggregation is required in the wetter East region and the upper areas of the Cordillera Central (in the middle of the island). In contrast, the hydrologic variables require fewer days of aggregation in the wetter areas. Given these results, this study presents the island-wide hydrologic projections as annual averages.

The KS tests showed large regional differences in the ability of the different GCMs used for the ARRM-driven models to reproduce the MSD-driven models. A set of 'best flow GCMs' in each region was determined from those that met the criteria of p-values of 0.01 or greater for all flow variables (total, surface, subsurface, and groundwater flow) in at least 75% of the region, for 1 year or less of temporal aggregation. The ensemble of 'best flow GCMs' is made up of GFDL_2.1 and HADCM3 in the North region; CCSM, CNRM, GFDL_2.1, HADCM3, and PCM in the South region; and CCSM, CGCM3_T63, CNRM, ECHAM5, and ECHO in the East region. The West region did not have any GCMs that met the KS test criteria.

4.2. Model results by climate region

By the end of the 21st century, the projected climatic changes on the island result in declining streamflow (and the components of total flow) for both emission scenarios and regardless of the make-up of climate model ensemble for each region (Figure 7, Table 2). However, the streamflow declines are more severe and exhibit greater uncertainty for the A2 emissions scenario. In all regions the total flow for the A2 scenario had a slightly larger range of model results compared with the lower emission scenario of B1. The complete GCM ensemble tended to have more flow than the ensembles of 'best flow GCMs' and 'bimodal precipitation GCMs'. On average, the percentage of the historical mean for total flow is 6% and 25% higher at the end of the century for 'best flow GCMs' and 'bimodal precipitation GCMs', respectively (Figure 7). Overall, the projected change in the ensemble average of all GCMs for total flow decreases from the 1960s to the 2090s by 49–88% of the historical amounts for scenario A2 and by 39–79% for scenario B1 (Table 2).

While consistent declining trends in total flow are evident, the individual flow component responses that are responsible for total flow varied by region and emissions scenario (Table 2). Note, the accuracy of these component responses is difficult to evaluate because only total flow is measured by the stream gage observations. Nevertheless, in general the modelled response of the subsurface flow component decreases the least as a percentage of the historical mean and the groundwater flow component decreases the most. The East region had the smallest projected changes and the North region had the largest. The A2 scenario ensemble had on average 9% more decrease from historical means than the B1 scenario ensembles, in each region and component. The fraction that each component contributes to total flow is also reported in Table 2. Surface flow is the biggest contributor in all regions except the West region (where groundwater flow is modelled as the most important component-contributor to total flow). Over the projected period, the fractions from surface flow

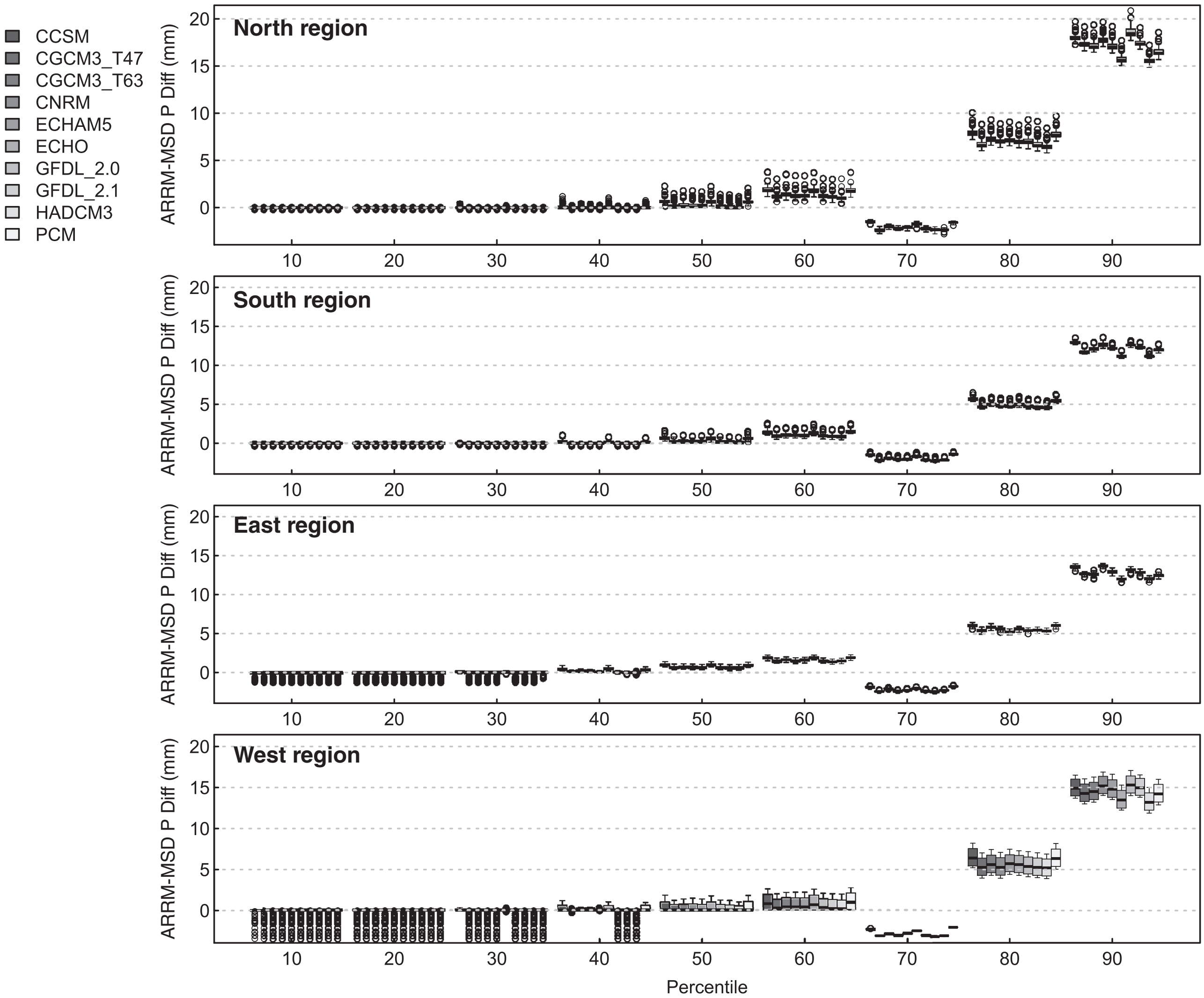

Figure 5. Range in HRU bias in the mean daily precipitation values by percentile (ARRM-MSD), for the North, South, East, and West regions.

and subsurface flow increased, and the fraction of groundwater flow decreased across Puerto Rico. The fractions of the flow components in the historical period (1962–2012) of the ARRM models are comparable with those from the MSD models (values not shown in Table 2). For more details on the time series of the projected flow components see Figures S7–S10.

The regional hydrological differences projected by the model (the East region had the smallest projected changes and the North region had the largest) are not a result of differences amongst the regions in the magnitude or timing of projected climate change. An analysis of the ARRM outputs shows similar changes at the stations in each region, with increases of 5–8°C from the 1960s to the 2090s in projected maximum daily temperature, increases of 6–11°C in projected minimum daily temperature, and decreases of 25–35% of historical amounts in projected daily precipitation, under B1 and A2 emission scenarios respectively. These projected changes are propagated through the environmental system in each region differently resulting in different projected effects on the hydrological regime in each region.

4.3. Results for critical water supply locations

The inferred mean withdrawals upstream of the gage for Lago La Plata were 3.03 and 24.01 $m^3 s^{-1}$ for Lago Loíza. These estimates were derived from averaging the difference between the measured gage data that include all upstream and reservoir withdrawals and the simulated data with no withdrawals included, for the period 1990–2012 for Lago La Plata, and for the period 1988–2007 and 2009–2012 for Lago Loíza (Figure 4). Estimates also discounted model error and reservoir evaporation loss, and assumed that differences between simulated and measured streamflow were due to upstream and reservoir withdrawals (or additions). Based on these estimates, there is a combined total average withdrawal of 27.04 $m^3 s^{-1}$ for the overlap period of years 1990–2012. For the historical period of annual water consumption growth rate, this study used the estimate of 4.3% taken from the Larsen (2000) calculation over the 1960–1997 Puerto Rico period. For the future period, this study used a conservative estimate of 0.3% increase per year based on projected population increases and

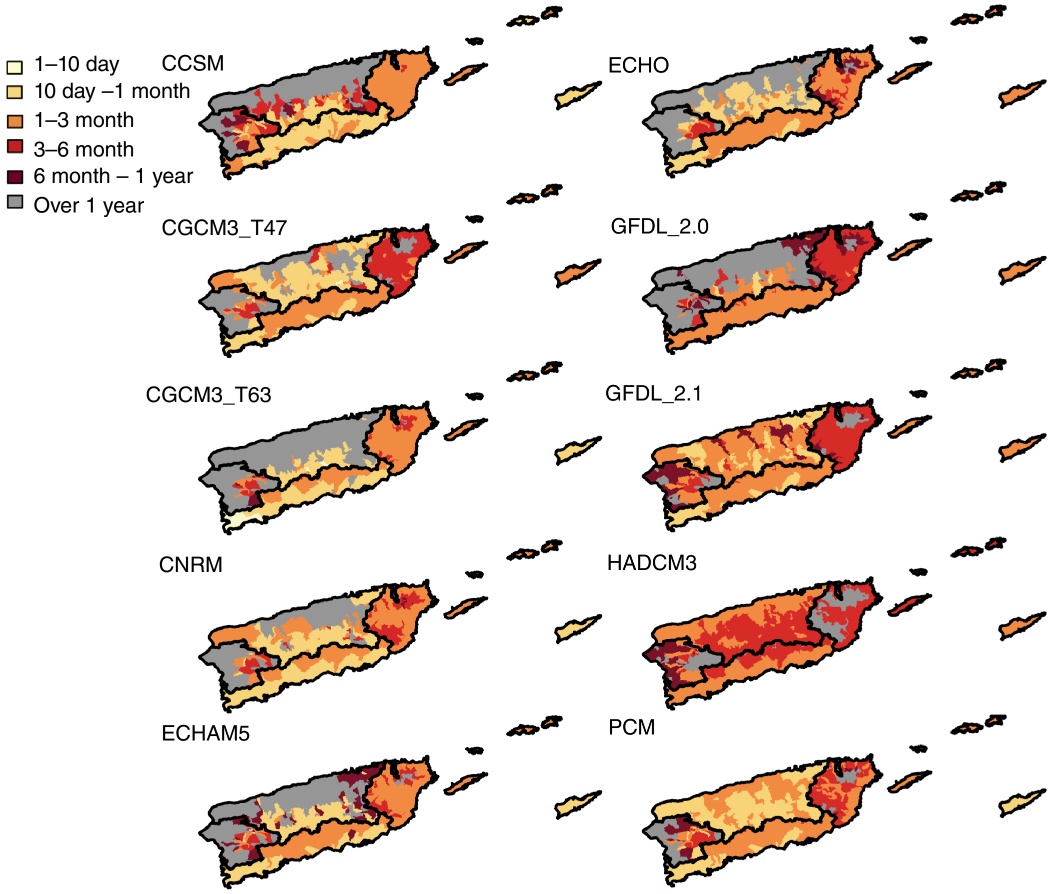

Figure 6. Number of days of data aggregation to accept the KS test null hypothesis that ARRM and MSD are from identical populations, for the total flow variable and each GCM. Black lines outline the four regions. The full figure for all variables and GCMs is Figure S6.

business as usual scenarios of water consumption (Hejazi *et al.*, 2013).

Using these estimated withdrawals, annual streamflow leaving the reservoirs of Lago La Plata and Lago Loíza is projected to decrease to zero by 2025 under the A2 emissions scenario and 2040 under the B1 emissions scenario (Figure 8). Deficits continue to increase through the remainder of the century. The amount leaving the reservoirs was calculated by subtracting the estimated withdrawals from the simulated streamflow for both the PRMS-MSD and PRMS-ARRM. Note that Lago La Plata is in the North region and Lago Loíza is in the East region, therefore the GCM members in the 'best flow GCMs' ensembles will vary depending on the KS test results.

5. Discussion

5.1. Sources of biases in hydrologic model results

Climate model simulations of temperature are typically highly correlated with observations, and statistical downscaling techniques have been shown to successfully model local-scale conditions in the tropics (Fowler *et al.*, 2007; Buytaert *et al.*, 2009). Thus, it is not surprising that the spatially distributed temperatures in the models using MSD and ARRM have similar empirical distributions. However, precipitation is difficult to model in tropical island systems (Douville *et al.*, 2006). Hydrology in Puerto Rico is more influenced by daily precipitation than temperature so biases in precipitation will more strongly affect the accuracy of the hydrologic modelling.

Gutmann *et al.* (2014) found that ARRM is very sensitive to GCM representation of precipitation; in particular, the distribution of precipitation by ARRM is expected to be spatially and temporally smoothed from the truth. The steep precipitation gradients on tropical islands lead to different patterns of hydrologic flow interannual variability across the regions that may be inaccurately represented by the ARRM-driven models. It is noticeable that the interannual variability of the hydrologic variables from the ARRM-driven models is much more similar across the regions than the hydrologic variables from the MSD-driven models are (Figure 7, for component details see Figures S7–S11).

The smoothing of precipitation by GCMs is exhibited in the tendency of GCMs to simulate constant drizzle (Dai, 2006). This is a probable reason for the ARRM overestimation of the smaller precipitation events as shown in Figure 5. Also in Figure 5, the ARRM underestimation of extreme events (e.g. hurricanes) is shown. The poor modelling of hurricanes is a known problem of statistical downscaling (see Sunyer *et al.*, 2012). These biases propagate

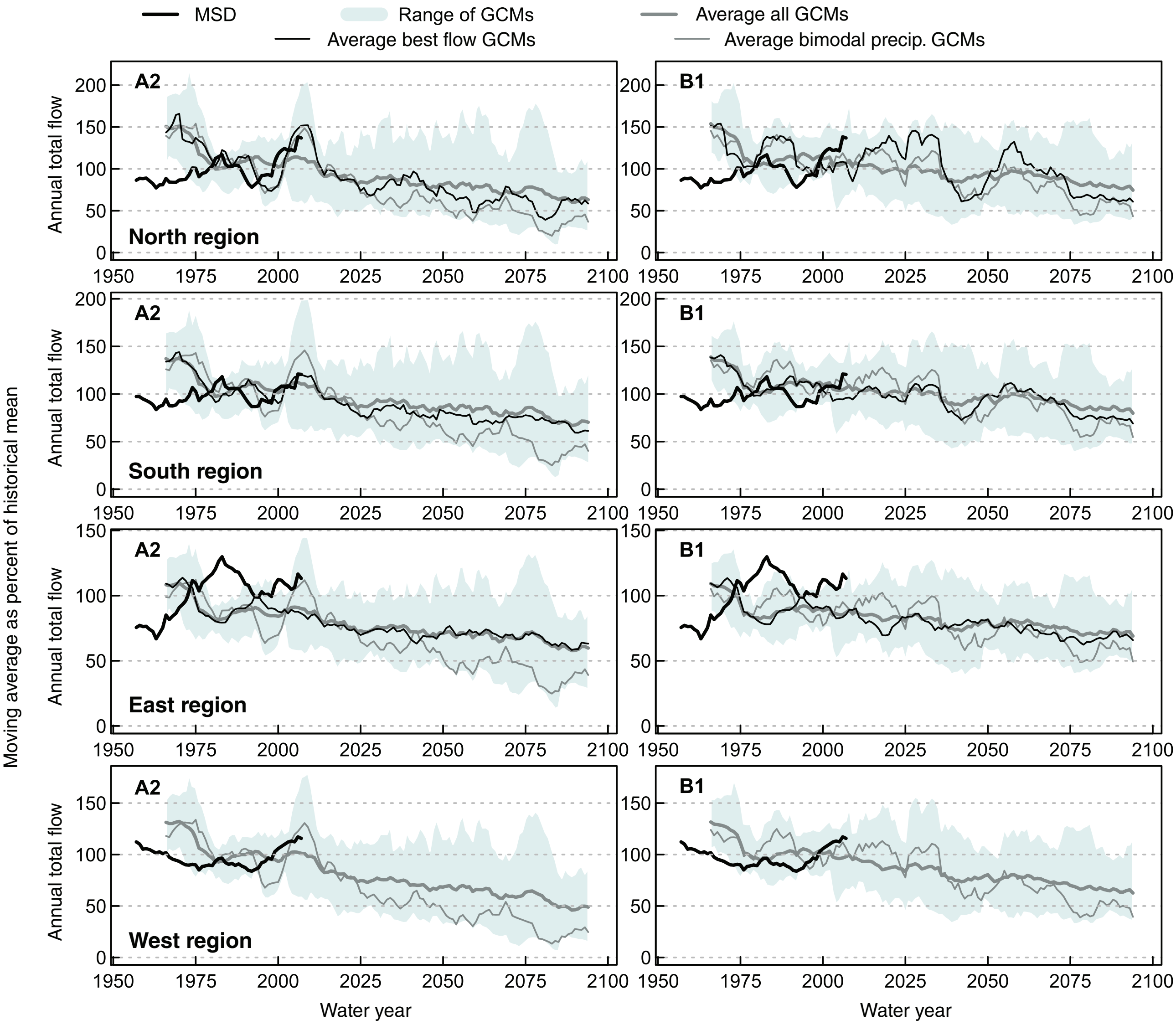

Figure 7. Ten-year moving averages of annual simulated total flow as percent of simulated historical mean (mean of using MSD 1953–2012) using MSD, range of GCMs, and multi-model GCM ensembles for the North, South, East, and West regions.

through the flow variables and result in truncated distributions that are less positively skewed than the MSD (except in the case of groundwater). The larger variance, more positive skew, and larger kurtosis in the ARRM-driven models of groundwater compared with the MSD-driven models is likely caused by: (1) positive bias in the small precipitation events which are not large enough to percolate into the groundwater reservoir, and (2) positive bias in the large precipitation events which cannot cause equally large groundwater flow events due to limited capacity of the groundwater reservoir (Scholl and Murphy, 2014).

5.2. Implications of temporal resolution for projections

The KS tests of the historic observed and modelled hydrology showed that region-wide projections cannot be expected to be accurate on temporal scales of less than a year. This is not surprising given the difficulties in modelling the climate in the tropics with sparse data and complicated climate dynamics. Ryu and Hayhoe (2013) found that only two GCMs of the ten used for this study were able to accurately simulate the NASH over the Caribbean and thus model the timing and magnitude of the bimodal seasonal cycle of precipitation. The results of this study strongly suggest that the downscaled projections from these GCMs cannot be used to support inferences about future seasonal changes in the hydrologic regime of Puerto Rico. As more downscaled ensembles (based on both statistical and dynamical downscaling) become available, more robust estimates of the uncertainty from the downscaling will be possible (Mizukami *et al.*, 2015). The findings here highlight the need for other studies examining climate change impacts on tropical hydrological regimes to take into account these issues of appropriate temporal resolution before drawing conclusions. Because short-term seasonal changes are not an overwhelming issue for reservoirs with storage capacity, the downscaled projections could be used to make useful conclusions about future water supply.

Table 2. Projected changes in amount and contributions of flow components for ensemble of all GCMs.

Region	Change in percent of historical mean at from 1960s to end of 21st century*							
	Total flow		Surface flow		Subsurface flow		Groundwater flow	
	A2	B1	A2	B1	A2	B1	A2	B1
North	−88%	−79%	−72%	−67%	−61%	−52%	−173%	−155%
	Fraction of total flow†		0.48–0.50	0.48–0.49	0.25–0.35	0.25–0.33	0.27–0.15	0.27–0.18
South	−67%	−59%	−63%	−54%	−42%	−44%	−167%	−160%
	Fraction of total flow†		0.78–0.78	0.78–0.80	0.11–0.15	0.11–0.13	0.11–0.07	0.11–0.07
East	−49%	−39%	−45%	−35%	−35%	−42%	−96%	−83%
	Fraction of total flow†		0.77–0.78	0.77–0.80	0.10–0.14	0.11–0.11	0.13–0.08	0.12–0.09
West	−82%	−69%	−69%	−59%	−110%	−99%	−96%	−71%
	Fraction of total flow†		0.34–0.43	0.34–0.39	0.13–0.17	0.13–0.15	0.53–0.40	0.53–0.46

*Difference between first and last calculated 10-year moving average.
†Component's fraction of total flow from year of first calculated 10-year moving average to last.

Temporal resolution was found to be highly variable by geographic area. More days of aggregation are needed in the wetter areas to simulate the precipitation distributions but fewer days of aggregation are needed in the wetter areas to simulate the hydrologic variables (for more details see Figure S6). This suggests that although large precipitation events are not well-simulated by the ARRM, the hydrologic model is increasingly less sensitive to exact amounts of precipitation as the overall amount of precipitation increases. If so, then future improvements in simulating precipitation would provide the greatest benefit in the drier South region. Hurricanes and other large storms embedded in the trade winds deliver about 70% of yearly rainfall on the island as a whole (Murphy and Stallard, 2012), therefore using a downscaling method that simulated hurricanes could greatly improve hydrologic modelling in the South.

5.3. Uncertainty in choosing the best climate model

The structural uncertainty across the GCMs is typically the largest source of hydrologic change uncertainty; larger than the uncertainty arising from deficiencies in the hydrologic model and the downscaling method (Fowler *et al.*, 2007; Buytaert *et al.*, 2009), and this problem is most evident in the tropics (Douville *et al.*, 2006). Choosing an ensemble such as 'best flow GCMs' by reproducibility of historical modelled variables is recommended by some authors (e.g. Knutti, 2010). It is interesting that the set of 'best flow GCMs' was different in each climatic region, showing that attempts to use model weighting and model culling to derive more accurate projections may not be robust. This is a well-known problem with model weighting and stems from the fact that there is not necessarily a relationship between: (1) the quality of the model physics determining regional temperature and precipitation, (2) the quality of the empirical ARRM method, and (3) the quality of the model physics that determine the estimated climate sensitivity to anthropogenic greenhouse gas emissions (Pierce *et al.*, 2009). The uncertainty propagated through the modelling chain of GCM to ARRM to HRU climate inputs to PRMS hydrologic model may be enhanced or compensated for, with different components cancelling the errors (Pappenberger and Beven, 2006). This may be another explanation for the seemingly contradictory results of poor simulation of precipitation in wetter areas by the ARRM, but lower errors when modelling the flow variables (for more details see Figure S6).

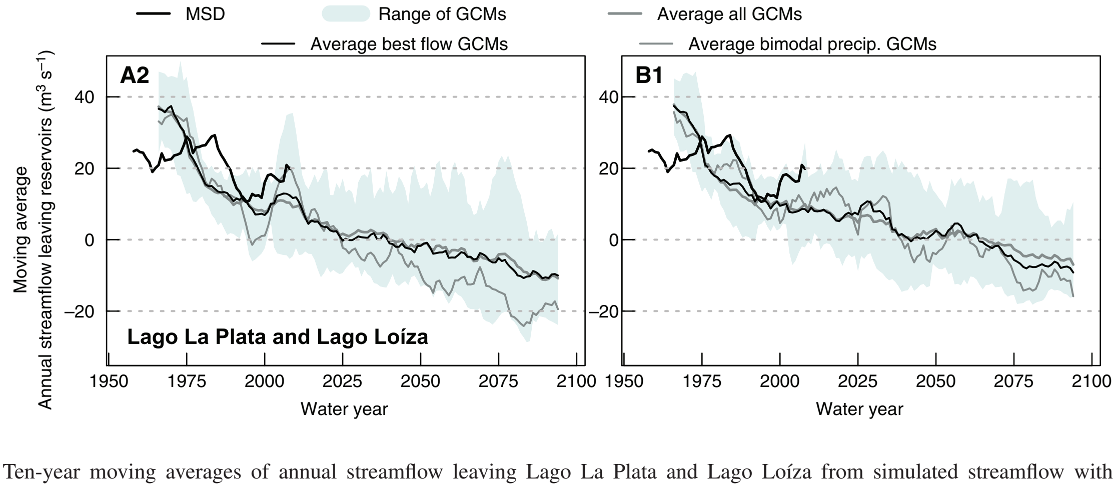

Figure 8. Ten-year moving averages of annual streamflow leaving Lago La Plata and Lago Loíza from simulated streamflow with estimated withdrawals subtracted using MSD, range of GCMs, and multi-model GCM ensembles.

5.4. Uncertainty in hydrologic model structures and parameters

This study uses only a single model structure (PRMS) and a single set of model future parameter values for the assessment of hydrologic changes. There is uncertainty in these choices that might have substantial effects when quantifying climate change impacts (e.g. changes in overall water balance, individual storages and fluxes, hydrologic signature measures, see Surfleet *et al.*, 2012 and Mendoza *et al.*, 2015). The hydrologic model used in this study has multi-objective calibration (Mendoza *et al.*, 2015) and historical (albeit not future) dynamic land cover parameters (Surfleet *et al.*, 2012), both suggested to reduce some of the uncertainty introduced by using only one hydrologic model. Future work should more carefully examine the effect of different hydrologic model structures and model parameter values on the projected flow regimes.

5.5. Unknown uncertainty from human impacts

Human impacts not considered here will change future flow. Most projected land cover change in Puerto Rico (as well as the tropics as a whole) is in the direction of urban expansion (Velazquez-Lozada *et al.*, 2006), which affects future flow amounts (Van Beusekom *et al.*, 2014). Urban expansion also affects useable water supply amounts, because it can easily tax water supply management systems beyond their capabilities to control water pollution and leaky networks (Bonell *et al.*, 2005). Furthermore, human reductions of streamflow component sources will affect regional total flow and specific location streamflow. As with many tropical islands, a portion of the water supply in Puerto Rico is taken directly from groundwater (White and Falkland, 2010). If the groundwater is pumped elsewhere and therefore not able to contribute to streamflow, the total flow will decrease.

5.6. Implications for future water supply

The results show that after accounting for uncertainty in the downscaled climate model ensemble, substantial losses of freshwater resources would be likely in upcoming decades under the two greenhouse gas emissions scenarios used in this study. This has implications for domestic, agricultural, industrial and energy uses as well as sustainable ecosystem function. A forward-looking management response may have to consider difficult tradeoffs, including calculated use of diminishing resources and an appropriate balance of uses. This analysis indicates projected changes for any watershed will depend on the watershed size, land cover, characteristics of precipitation events and water management, as illustrated by the results on the future of Lago La Plata and Lago Loíza, as well as the variation in the regional results. A very small increase per year in water consumption (even an increase less than the 0.3% per year considered here) compounded with a large decrease in available water regionally on already overtaxed reservoirs would likely lead to water shortages. Finally, the projected decrease in total flow of 60–70% of historic amounts shows that the effects on water supply are not likely to correspond in a simple linear manner to changes in precipitation or temperature, as this is considerably larger than the projected changes in climate emphasizing the potential for compounded effects of climate change in the tropics (Wohl *et al.*, 2012). Further exploration of the projected streamflow on the island will be useful for highlighting those watersheds and water-dependent resources at greatest risk.

6. Conclusions

In order to study the challenges of projecting the effects of climate change on limited water resources of tropical islands, this study used the island of Puerto Rico with a previously configured hydrologic model and an ensemble of statistically downscaled GCM models. The large differences between the hydrologic models driven with downscaled GCM output versus the models driven with MSD highlighted the difficulties in modelling areas with the sparse climate data and steep precipitation gradients typical of tropical islands. As long as model uncertainty is assessed, implications of the projected hydrology on future water resources are valuable as they are the current best available projections of future streamflow and surface water resources.

Based on the uncertainty analysis, the temporal resolution of the projected hydrologic flow variables in Puerto Rico was calculated on an annual scale. The range of projected total flows using all available GCMs was up to 1.5 times the magnitude of historical mean flows, but the full and reduced-size ensembles both showed decreases in annual total flow after 2025. From the 1960s to the 2090s, the magnitudes of total flow from the GCM ensembles decreased across Puerto Rico by ~70–60% of historical amounts under A2 and B1 emission scenarios, respectively. Subsurface flow contributions decreased the least by percentage of historical mean and groundwater flow contributions decreased the most, leading to the fraction of flow coming from subsurface flow to increase and the fraction of flow coming from groundwater flow to decrease. The smallest projected changes were in the East region and the largest in the North region. Much work remains to evaluate additional sources of uncertainty, most importantly, potential future human impacts on future hydrology and water resources in tropical islands. Nevertheless, this study illustrates a method of estimating the timing of hydrological regime changes that would result in substantial negative consequences for freshwater supplies. At locations critical to water supply in Puerto Rico, projected streamflow is likely to decrease below projected withdrawals by the middle of the century and perhaps be in a deficit of 10 to 20 $m^3 s^{-1}$ by 2099.

Acknowledgements

This research supported in part by the Caribbean Landscape Conservation Cooperative. We would like to thank our anonymous reviewers. Any use of trade, product, or firms names is for descriptive purposes only and does not imply endorsement by the U.S. government. All research at the US FS International Institute of Tropical Forestry is done in collaboration with the University of Puerto Rico.

Supporting Information

The following supporting information is available as part of the online article:

Figure S1. Annual simulated flow components using MSD and dynamic land cover parameters for the North, South, East, and West regions.

Figure S2. Range in HRU bias and percent bias in the mean daily values (ARRM-MSD) for each variable for all regions combined.

Figure S3. Range in HRU bias and percent bias in the variance in daily values (AARM-MSD) for each variable for all regions combined.

Figure S4. Range in HRU bias and percent bias in the skewness in daily values (ARRM-MSD) for each variable for all regions combined. Thirty outliers in groundwater flow are off the plot positively to 1500, and 10 are off the plot negatively to −1000.

Figure S5. Range in HRU bias and percent bias in the kurtosis in daily values (ARRM-MSD) for each variable for all regions combined.

Figure S6. Number of days of data aggregation to accept the KS test null hypothesis that ARRM and MSD are from identical populations, for each variable and GCM. Black lines outline the four regions.

Figure S7. Ten-year moving averages of annual simulated flow components as percent of simulated historical mean (mean of using MSD 1953-2012) using MSD, range of GCMs, and multi-model GCM ensembles for the North region.

Figure S8. Ten-year moving averages of annual simulated flow components as percent of simulated historical mean (mean of using MSD 1953-2012) using MSD, range of GCMs, and multi-model GCM ensembles for the South region.

Figure S9. Ten-year moving averages of annual simulated flow components as percent of simulated historical mean (mean of using MSD 1953-2012) using MSD, range of GCMs, and multi-model GCM ensembles for the East region.

Figure S10. Ten-year moving averages of annual simulated flow components as percent of simulated historical mean (mean of using MSD 1953-2012) using MSD, range of GCMs, and multi-model GCM ensembles for the West region. There are no best flow GCMs for the region.

References

Addor N, Rössler O, Köplin N, Huss M, Weingartner R, Seibert J. 2014. Robust changes and sources of uncertainty in the projected hydrological regimes of Swiss catchments. *Water Resour. Res.* **50**: 7541–7562.

Alcamo J, Flörke M, Märker M. 2007. Future long-term changes in global water resources driven by socio-economic and climatic changes. *Hydrol. Sci. J.* **52**: 247–275.

Angeles ME, Gonzalez JE, Erickson DJ, Hernández JL. 2007. Predictions of future climate change in the Caribbean region using global general circulation models. *Int. J. Climatol.* **27**: 555–569.

Angulo J, Jenkins A, Lebedev A, McNeff N. 2011. *Assessing the Lifespans of Reservoirs in Region 2 of Puerto Rico*. The Conservation Trust of Puerto Rico: San Juan, 82 pp.

Benstead JP, March JG, Pringle CM, Scatena FN. 1999. Effects of a low-head dam and water abstraction on migratory tropical stream biota. *Ecol. Appl.* **9**: 656–668.

Bonell M, Hufschmidt MM, Gladwell JS. 2005. *Hydrology and Water Management in the Humid Tropics: Hydrological Research Issues and Strategies for Water Management*. Cambridge University Press: Cambridge, UK.

Buytaert W, Célleri R, Timbe L. 2009. Predicting climate change impacts on water resources in the tropical Andes: effects of GCM uncertainty. *Geophys. Res. Lett.* **36**: L07406.

Carter M, Elsner J. 1997. A statistical method for forecasting rainfall over Puerto Rico. *Weather Forecast.* **12**: 515–525.

Chen H, Xu C-Y, Guo S. 2012. Comparison and evaluation of multiple GCMs, statistical downscaling and hydrological models in the study of climate change impacts on runoff. *J. Hydrol.* **434–435**: 36–45.

Cintron G, Lugo AE, Pool DJ, Morris G. 1978. Mangroves of arid environments in Puerto Rico and adjacent islands. *Biotropica* **10**: 110–121.

Conover W. 1971. *One-Sample "Kolmogorov" Test/Two-sample "Smirnov" Test. Practical Nonparametric Statistics*. John Wiley & Sons: New York, NY, 295–301.

Cooney PB, Kwak TJ. 2013. Spatial extent and dynamics of dam impacts on tropical island freshwater fish assemblages. *Bioscience* **63**: 176–190.

Dai A. 2006. Precipitation characteristics in eighteen coupled climate models. *J. Clim.* **19**: 4605–4630.

Daly C, Helmer EH, Quiñones M. 2003. Mapping the climate of Puerto Rico, Vieques and Culebra. *Int. J. Climatol.* **23**: 1359–1381.

Douville H, Salas-Mélia D, Tyteca S. 2006. On the tropical origin of uncertainties in the global land precipitation response to global warming. *Clim. Dyn.* **26**: 367–385.

Fowler HJ, Blenkinsop S, Tebaldi C. 2007. Linking climate change modelling to impacts studies: recent advances in downscaling techniques for hydrological modeling. *Int. J. Clim.* **27**: 1547–1578.

Giannini A, Kushnir Y, Cane MA. 2000. Interannual variability of Caribbean rainfall, ENSO, and the Atlantic Ocean. *J. Clim.* **13**: 297–311.

Gutmann E, Pruitt T, Clark MP, Brekke L, Arnold JR, Raff DA, Rasmussen RM. 2014. An intercomparison of statistical downscaling methods used for water resource assessments in the United States. *Water Resour. Res.* **50**: 7167–7186.

Harmsen E, Gonzalez-Perez A, Winter A. 2004. Re-evaluation of pan evaporation coefficients at seven locations in Puerto Rico. *J. Agric. Univ. P. R.* **88**: 109–122.

Hay LE, Umemoto M. 2006. Multiple-objective stepwise calibration using Luca. U.S. Geological Survey Open-File Report 2006–1323, Reston, VA.

Hay LE, Leavesley GH, Clark MP, Markstrom SL, Viger RJ, Umemoto M. 2006. Step wise, multiple objective calibration of a hydrologic model for a snowmelt dominated basin. *J. Am. Water Resour. Assoc.* **42**: 877–890.

Hay LE, LaFontaine J, Markstrom SL. 2014. Evaluation of statistically downscaled GCM output as input for hydrological and stream temperature simulation in the Apalachicola–Chattahoochee–Flint River Basin (1961–99). *Earth Interact.* **18**: 1–32.

Hejazi M, Edmonds J, Chaturvedi V, Davies E, Eom J. 2013. Scenarios of global municipal water-use demand projections over the 21st century. *Hydrol. Sci. J.* **58**: 519–538.

Hunter JM, Arbona SI. 1995. Paradise lost: an introduction to the geography of water pollution in Puerto Rico. *Soc. Sci. Med.* **40**: 1331–1355.

Huntington TG. 2006. Evidence for intensification of the global water cycle: review and synthesis. *J. Hydrol.* **319**: 83–95.

Knutti R. 2010. The end of model democracy? *Clim. Change* **102**: 395–404.

Koenker R, Bassett G Jr. 1978. Regression quantiles. *Econometrica* **46**: 33–50.

Larsen MC. 2000. Analysis of 20th century rainfall and streamflow to characterize drought and water resources in Puerto Rico. *Phys. Geogr.* **21**: 494–521.

Leavesley GH, Lichty RW, Troutman BM, Saindon LG. 1983. Precipitation-runoff modeling system – user's manual. U.S. Geological Survey Water-Resources Investigations Report 83-4238, Reston, VA.

Markstrom SL, Niswonger RG, Regan RS, Prudic DE, Barlow PM. 2008. GSFLOW, coupled ground-water and surface-water flow model based on the integration of the Precipitation-Runoff Modeling System (PRMS) and the Modular Ground-Water Flow Model (MODFLOW-2005). U.S. Geological Survey Techniques and Methods 6-D1, Reston, VA, 240 pp.

Mendoza PA, Clark MP, Mizukami N, Newman AJ, Barlage M, Gutmann ED, Rasmussen RM, Rajagopalan B, Brekke LD, Arnold JR. 2015. Effects of hydrologic model choice and calibration on the portrayal of climate change impacts. *J. Hydrometeorol.* **16**: 762–780.

Mielke PW, Johnson ES. 1974. Some generalized beta distributions of the second kind having desirable application features in hydrology and meteorology. *Water Resour. Res.* **10**: 223–226.

Mizukami N, Clark M, Gutmann E, Mendoza P, Newman A, Nijssen B, Livneh B, Hay L, Arnold J, Brekke L. 2015. Implications of the methodological choices for hydrologic portrayals of climate change over the Contiguous United States: statistically downscaled forcing data and hydrologic models. *J. Hydrometeorol.* doi: http://dx.doi.org/10.1175/JHM-D-14-0187.1 (accessed 9 March 2015)

Molina-Rivera WL, Gómez-Gómez F. 2008. Estimated water use in Puerto Rico, 2005. U.S. Geological Survey Open-File Report 2008–1286, Reston, VA, 37 pp.

Murphy SF, Stallard RF. 2012. Chapter C: Hydrology and climate of four watersheds in Eastern Puerto Rico. In *Water Quality and Landscape Processes of Four Watersheds in Eastern Puerto Rico, U.S. Geological Survey Professional Paper 1789-C*, Murphy SF, Stallard RF (eds). USGS: Reston, VA, 43–84.

Nakicenovic N, Alcamo J, Davis G, de Vries B, Fenhann J, Gaffin S, Gregory K, Grubler A, Jung TY, Kram T, La Rovere EL, Michaelis L, Mori S, Morita T, Pepper W, Pitcher HM, Price LM, Riahi K, Roehrl A, Rogner H-H, Sankovski A, Schlesinger M, Shukla P, Smith SJ, Swart R, van Rooijen S, Victor N, Dadi Z. 2000. *Special Report on Emissions Scenarios: A Special Report of Working Group III of the Intergovernmental Panel on Climate Change*. Pacific Northwest National Laboratory/Environmental Molecular Sciences Laboratory: Richland, WA.

Neal JW, Lilyestrom CG, Kwak TJ. 2009. Factors influencing tropical island freshwater fishes: species, status, and management implications in Puerto Rico. *Fisheries* **34**: 546–554.

Pappenberger F, Beven KJ. 2006. Ignorance is bliss: or seven reasons not to use uncertainty analysis. *Water Resour. Res.* **42**: W05302.

Pierce DW, Barnett TP, Santer BD, Gleckler PJ. 2009. Selecting global climate models for regional climate change studies. *Proc. Natl. Acad. Sci. U.S.A.* **106**(21): 8441–8446.

Præstgaard JT. 1995. Permutation and bootstrap Kolmogorov-Smirnov tests for the equality of two distributions. *Scand. J. Stat.* **22**: 305–322.

Ryu J-H, Hayhoe K. 2013. Understanding the sources of Caribbean precipitation biases in CMIP3 and CMIP5 simulations. *Clim. Dyn.* **42**: 3233–3252.

Scholl MA, Murphy SF. 2014. Precipitation isotopes link regional climate patterns to water supply in a tropical mountain forest, eastern Puerto Rico. *Water Resour. Res.* **50**(5): 4305–4322.

Stainforth DA, Downing TE, Washington R, Lopez A, New M. 2007. Issues in the interpretation of climate model ensembles to inform decisions. *Philos. Trans. R. Soc. Math. Phys. Eng. Sci.* **365**: 2163–2177.

Stoner AMK, Hayhoe K, Yang X, Wuebbles DJ. 2013. An asynchronous regional regression model for statistical downscaling of daily climate variables. *Int. J. Climatol.* **33**: 2473–2494.

Sunyer MA, Madsen H, Ang PH. 2012. A comparison of different regional climate models and statistical downscaling methods for extreme rainfall estimation under climate change. *Atmos. Res.* **103**: 119–128.

Surfleet CG, Tullos D, Chang H, Jung I-W. 2012. Selection of hydrologic modeling approaches for climate change assessment: A comparison of model scale and structures. *J. Hydrol.* **464–465**: 233–248.

Terando A, Keller K, Easterling WE. 2012. Probabilistic projections of agro-climate indices in North America. *J. Geophys. Res.* **117**: D08115.

Todd MC, Taylor RG, Osborn TJ, Kingston DG, Arnell NW, Gosling SN. 2011. Uncertainty in climate change impacts on basin-scale freshwater resources – preface to the special issue: the QUEST-GSI methodology and synthesis of results. *Hydrol. Earth Syst. Sci.* **15**: 1035–1046.

Van Beusekom AE, Hay LE, Viger RJ, Gould WA, Collazo JA, Henareh Khalyani A. 2014. The effects of changing land cover on streamflow simulation in Puerto Rico. *J. Am. Water Resour. Assoc.* **50**(6): 1575–1593.

Vano JA, Udall B, Cayan DR, Overpeck JT, Brekke LD, Das T, Hartmann HC, Hidalgo HG, Hoerling M, McCabe GJ, Morino K, Webb RS, Lettenmaier DP. 2014. Understanding uncertainties in future Colorado River streamflow. *Bull. Am. Meteorol. Soc.* **95**: 59l.A.

Velazquez-Lozada A, Gonzalez JE, Winter A. 2006. Urban heat island effect analysis for San Juan, Puerto Rico. *Atmos. Environ.* **40**(9): 1731–1741.

Viger RJ, Bock A. 2014. GIS features of the geospatial fabric for national hydrologic modeling. U.S. Geological Survey Techniques and Methods: Reston, VA, 201 pp.

Vrac M, Naveau P. 2007. Stochastic downscaling of precipitation: from dry events to heavy rainfalls. *Water Resour. Res.* **43**: W07402.

White I, Falkland T. 2010. Management of freshwater lenses on small Pacific islands. *Hydrogeol. J.* **18**: 227–246.

Wilby RL, Harris I. 2006. A framework for assessing uncertainties in climate change impacts: low-flow scenarios for the River Thames, UK. *Water Resour. Res.* **42**: W02419.

Wohl E, Barros A, Brunsell N, Chappell NA, Coe M, Giambelluca T, Goldsmith S, Harmon R, Hendrickx JMH, Juvik J, McDonnell J, Ogden F. 2012. The hydrology of the humid tropics. *Nat. Clim. Change* **2**: 655–662.

Zhao M, Held IM, Lin S-J, Vecchi GA. 2009. Simulations of global hurricane climatology, interannual variability, and response to global warming using a 50-km resolution GCM. *J. Clim.* **22**: 6653–6678.

